Climate Change Impacts on Broussonetia papyrifera Pollen - Metabolome Investigations and Prospects of Allergy Prevalence in Times of Climate Change

Muhammad Humayun
COMSATS University Islamabad
Saadia Naseem
COMSATS University Islamabad
Zahid Ali (zahidali@comsats.edu.pk)
COMSATS University Islamabad
Richard E. Goodman
University of Nebraska–Lincoln

Research Article

Keywords: B. papyrifera Pollen, FTIR, LCMS, Climate change

Posted Date: March 16th, 2023

DOI: https://doi.org/10.21203/rs.3.rs-2672801/v1

Abstract

Broussonetia papyrifera (*B. papyrifera*) is a tree producing allergenic pollen that grow at varied climatic conditions worldwide. The tree pollen disperse in the air causing allergies in susceptible humans. The study investigates climate change variable's impact on *B. papyrifera* pollen's composition, pollen metabolome, pollen allergenicity and their occurrence in the upcoming years. The tree pollens were collected in summer and spring from different regions in Pakistan. Pollens were subjected to morphological analysis, Fourier Transform Infrared Spectroscopy (FTIR), Liquid Chromatography-Mass Spectrometry (LCMS), and immunoblotting. The tree future-growth invasion was predicted through MaxEnt modeling. Light microscopy and FTIR showed seasonal and regional differences in pollen-morphology and pollen-metabolome that correlated to weather conditions' shift. LCMS analysis detected four allergenic lipids having a potential role in allergies. Pollen protein immunoblotting-studies identified putative 15 kDa novel allergen, and verified previously known 40 kDa, 33 kDa, and 10 kDa allergens*. B. papyrifera* MaxEnt modeling through ACCESS10 and CCSM4 under 2-greenhouse gas emissions scenarios {representative concentration pathway (RCP) 4.5 and 8.5} projected the tree invasion by the years 2050 and 2070. The study findings demonstrate that climatic variables differences affect *B. papyrifera*-pollen physiology. The study discovered allergenic lipids and a 15 kDa potential novel allergen in *B. papyrifera*-pollen protein extracts, and predicted the tree invasion in future. These results predict potential changes in *B. papyrifera*-pollen allergy risks in the future and provide a model system for studying pollen morphology, plant invasion, and associated allergies in response to climate changes for other species.

Introduction

Climate change is expected to have significant effects on plant growth and development, and could impact pollen seasons (Anderegg et al., 2021). Pollen size may be reduced, and smaller in size would remain in the air for longer periods, and are transported to longer distances (de Weger et al., 2016; Mohanty et al., 2017). Pollen has been widely studied in the fields of forensics, ecology, climate change, and aeroallergens investigations. There has been an increase in allergies as well as an increase in the amount of allergenic pollen throughout the world especially in the industrialized countries over the past 50 years (Damialis et al., 2019). It may be due to a lifestyle change of people, an increase in pollutant emissions, and an increase in allergenic pollen quantity in the air in distinct bioclimatic regions (Ziello et al., 2012). Industrialized countries have increased carbon dioxide emissions and other pollutant emissions that add to global warming. An increase in temperature and greater availability of carbon dioxide in the air favors the production of pollen in greater amounts (Schmidt, 2016). Variability in environmental factors induces changes in the chemical composition of lipids, carbohydrates, and proteins (Zimmermann et al., 2017) that may increase pollen allergies (Damialis et al., 2021). Higher temperature and elevated carbon and nitrogen metabolites affect pollen development (Santiago & Sharkey, 2019). Developing pollen needs a high amounts of membrane lipids and fatty acids (Ischebeck, 2016; Narayanan et al., 2018). Heat stress during pollen development affects pollen tube growth (Jiang et

al., 2017), and pollen appearance, pollen cell wall, and vesicular transport (Parrotta et al., 2016). Heat stress causes an early bursting of pollen tapetum layer responsible for pollen nutrition and development. These changes may alter allergenicity. Pollen are rich in mitochondria (Selinski & Scheibe, 2014), and oxidative damage in the tapetum layer of pollen adds to increased production of reactive oxygen species (ROS) that cause programmed cell death (Mittler, 2017). ROS activation causes the regulation of pollen-associated lipid metabolites (PALMs), and they have been known to evoke immune responses (Dahl, 2018). Phytoprostanes present in pollen (Traidl-Hoffmann et al., 2005) generate oxygen radicals. ROS in pollen catalyzes the production of oxylipids that yield a chain reaction by producing many unstable molecules that activate gene responses for enzymes responsible for external environment changes (Dahl, 2018). Average temperature variation of 1 ºC has been found to increase the pollen count of some plant species (Cupressaceae, Platanus, and Quercus) from 3000–9000 pollen grains/m^3 (Subiza et al., 2019) apart from changes in pollen composition. Climate change-induced variations in pollen composition may cause an increase in the allergenic potential of pollen.

Broussonetia papyrifera pollen is known to have a high allergenic potential (Aslam et al., 2015; Papia et al., 2020; Wu et al., 2019). Analysis of pollen protein extracts by skin prick test (SPT), and enzyme-linked immune sorbent assay (ELISA) identified 33-KDa and 40-KDa size proteins as potential allergens that may elicit allergenic responses in humans. While pollen of this species noted as causing urticaria and severe respiratory symptoms, the sequence identities of the IgE binding proteins have not been identified and allergenicity has not been confirmed. The tree is anemophilous (wind pollinated) in nature and produces large quantities of pollen having a size between 12–17 µm (Yang & Chen, 1998). According to the Global Biodiversity Forum (GBIF.org), *B. papyrifera* grows in Asia, in tropical and subtropical, and near equator regions. *B. papyrifera* was introduced into Pakistan in the early 1960s from East Asia for the beautification of Islamabad project (Aslam et al., 2015). There is variation in climatic factors in different regions of Pakistan (average temperature and precipitation) (Ajani & van der Geest, 2021; Saleem et al., 2021). *B. papyrifera*'s daily pollen count in Islamabad (district C) reaches 45000 pollen grains/m^3 in the spring season (http://www.pmd.gov.pk/rnd/rndweb/rnd_new/pr.php).

The pollen morphological and histological changes can be studied through microscopic techniques. However, changes in pollen lipids, proteins, and carbohydrates constituents and their correlation to allergy prevalence require molecular approaches to characterize proteins and lipids present in pollen. Variations in biochemical composition of pollen through Fourier Transform Infrared Spectroscopy (FTIR) is informative (Kenđel & Zimmermann, 2020). Kendel and Zimmermann have showed relative and absolute contents of lipids, carbohydrates, carotenoids, proteins and sporopollenins. The platform has been used as an easy and quick approach to study the biochemical structure of pollen where environmental stresses' effect on pollen pure samples (Zimmermann et al., 2017; Zimmermann & Kohler, 2014). Pollutants effect on pollen can intensify pollen allergic effects and induce allergies in humans (Depciuch et al., 2017). Similarly, liquid chromatography-mass spectrometry (LCMS) determines the presence of various chemical compounds in a sample by combining chromatography and mass spectrometry (Fragallah et al., 2018). The combined use of LCMS and FTIR tools help in studying variation in the

chemical composition of pollen in response to changes in temperature and precipitation. Thus, the current investigations aim to find inter-seasonal and inter-regional variations in *B. papyrifera* pollen under varied climatic conditions, and the the likely distribution of the plant in the years 2050 and 2070. It is pertinent to expedite research in factors associated with climate change and their possible influence on composition and allergenic properties of pollen.

Materials And Methods

Study area characteristics

The study area is comprised of regions having different geographical and climatic conditions – district Peshawar region 1 (R1), Islamabad region 2 (R2), and Kotli region 3 (R3). R1 is located at 331 m, R2 at 507 m, and R3 at 609 m elevation from sea level. The distance between R1 and R3 is 316 km; R1 and R2 is 187 km. and R2 and R3 is 132 km. Mean annual temperature during 2010–2020, for R1, R2 and R3 was 23.06°C, 21.39°C and 22.07°C respectively. Mean annual precipitation during this period was 42.31 mm, 110.34 mm and 102.445 respectively (https://www.pmd.gov.pk/en/). R2 and R3 have moderate environmental conditions in comparison to R3. All study regions have difference in geography and weather conditions (S1 Fig., S2 Fig.).

B. papyrifera **growth occurrence record**

B. papyrifera occurrence in Asia was downloaded (GBIF.org), and a field observation survey was carried out in the years 2020 and 2021 to record the occurrence of *B. papyrifera*. The locations were selected for pollen sampling with a minimum distance of 1 km away from one another. However, the nearest accessible location was recorded for plants growing in mountainous region where recording the exact location was difficult. Presence of the tree was recorded through the Google Earth Pro version 7.3 mobile application. Both GBIF.org occurrence data and field observations from Pakistan data showed the occurrence of 394 points dataset, in Microsoft excel sheet in species with data (SWD) in CSV format to build the MaxEnt model.

Pollen sampling

Pollen samples were collected from three *B. papyrifera* plants growing in a single district. Sampling was done from R1, R2 and R3 in the spring 2020 and 2021. Sterilized 50 mL tubes were used to store flowers in to avoid external sources of contamination of the pollen. The samples were dried for 72 hours in shade at room temperature. Dried pollen grains were released from the samples by tipping the dry panicle of *B. papyrifera* on a 500 μm pore size mesh. The isolated pollen grains were then passed through a 100 μm pore size mesh to collect pure pollen grains. The pure pollen samples were stored at room temperature (28°C) in 1.5 mL sterile tubes.

Microscopy of pollen samples

The microscopy of pollen samples was done following the protocol of Whitney & Needham (2014) with some modifications. The pollen from various areas and seasons were soaked in isopropanol for 10 minutes to extract lipids before applying them to glass slides (Whitney & Needham, 2014). A small drop of suspended pollen sample was put on the glass slide and allowed to dry. A drop of preheated glycerine (50°C) was added to the pollen inserted on the spot and covered with a glass coverslip before gently heating for 15 seconds to fix the pollen. The photographs of pollen were taken by ZEISS Axio Imager 2.0 light microscope, and exine lengths were calculated through Image J software https://imagej.nih.gov/ij/links.html.

Fourier transform infrared analysis of pollen

Samples of 20 mg of dried pollen grains taken from each sample, were placed on FTIR IRTracer-100 knob for analysis by following the protocol as described by (Kenđel & Zimmermann, 2020). Measurements were taken in triplicate with a Vertex 70v FT-IR Spectrometer using the attenuated total reflectance (ATR) method. Infrared radiations in the range of 500–4500 cm^{-1} and a resolution of 4 cm^{-1} were selected to draw peaks (Joanna Depciuch et al., 2018). The peaks were normalized and data files were imported in CSV format that was processed for drawing FTIR peaks through Origin pro 8.5E-2018 software.

Liquid chromatography-mass spectrometry (LCMS) analysis of pollen extracts

Samples of dried pollen (100 mg) were placed in 15 mL tubes with 2 mL of methanol as an extraction fluid and the tubes were kept on a shaker at room temperature for 1 hour. The extracts were passed through a SPE (Solid Phase Extraction) and samples were collected in 2.0 mL tubes. Pollen extracts were subjected to LC-MS/MS analysis as described by Kang et.al (Kang et al., 2020). An Agilent triple quadrupole system was used for LC-MS/MS where compounds were separated (model: G1776A, dimensions: 160 x 435 x 436 mm, temperature: 40˚C). The sample injection volume was 5 µL, and the mobile phase in A (100% acetonitrile) and solvent B (100% water). The mobile phase flow rate was 0.3 mL min^{-1} and the HPLC gradient contained 0–4 min. 2% A, 98% B; 4–7 min. 20% A, 80% B; 7–14 min. 90% A, 10% B; 15 min. 90% A, 10% B; 16 min. 2% A and 98% B. ESI positive mode by nitrogen gas was used for mass spectrometry where the gas temperature was 350°C, flow of gas 11 L min − 1, capillary voltage 4500 V, and nebulizer 50 psi to determine compounds by National Institute of Standards and Technology's (NIST 17) database.

Pollen protein extracts separated in SDS-PAGE followed by immunoblotting

Water-soluble pollen proteins were extracted in 1 X PBS buffer. Extracted proteins were quantified by Nano drop and using a 2D-Quant kit. Samples of 10-µg protein extract/well were separated in Novex 10–20% tris-glycine gels (Invitrogen, Carlsbad, CA, USA, Cat # EC61355. A 3 µl sample of pre-stained Precision Plus molecular weight marker proteins (Bio-Rad, Hercules, CA, USA, Cat # 161–0374) was loaded on each gel to allow the estimation of apparent molecular weight of the proteins. Protein extract

IgE binding from individual serum samples was confirmed by native immuno dot blot IgE binding activity of protein extracts with monoclonal mouse anti-human IgE conjugated with horseradish peroxidase (HRP) from Southern Biotech, Birmingham, AL (clone B3102E8 Cat #9160–05). Human serum samples were purchased from Plasma lab USA (supplementary table). Allergen confirmation was done through western blotting and immune-dot blots with selected serum samples. Protein extracts were pre-heated on 25°C, 70°C, and 95°C, cooled to room temperature, and then run on premade gels (Novex). Proteins were transferred to 0.45 µm nitrocellulose membranes (Invitrogen, Carlsbad, CA, USA, Cat # 645,239), and blocked with non-fat milk solution before applying diluted serum samples. Unbound IgE was removed by washing with 0.2% Tween 20 in PBS and followed by incubation with Southern Biotech's monoclonal anti-IgE coupled with horse radish peroxidase. The anti-IgE was visualized using Supersignal West Dura Extended Duration Chemiluminescent substrate (Pierce, Rockford, IL, USA, Cat # 34,076) in a UVP BioSpectrum 815 Imaging System for 1 minute and 5 minutes as described by (Ramadan et al., 2021).

Temperature, precipitation and spring maximum pollen count data analysis

Mean monthly temperature and precipitation data from 1991–2020 for R1 and R2, 2010–2020 for R3; and *B. papyrifera* spring maximum pollen count in a single day in one cubic meter in R2 was retrieved from PMD. Microsoft excel 2016 was used to make annual means of the data, and their plots.

MaxEnt Modeling

We have downloaded future climate data predictions of 19 Bioclimatic variables from WorldClim 1.4 (https://www.worldclim.com/CMIP5_30S) having 30-arc second resolution (0.93 × 0.93 km = 0.86 km^2 at the equator) for ACCESS1-0 and CCSM4 models for the years 2050 and 2070 RCP 4climate change scenario (Hijmans et al., 2005). Downloaded variable files were converted into Asc file format through QGIS 3.16.11. Bioclimatic variables were clipped onto the shapefile of Asia. These files were loaded on MaxEnt software version 3.4.4, and run as described by Phillips (Phillips, 2008). Accuracy assessments for all models were randomly divided into 25% and 75% to conduct random test and train the model. Background environmental data was applied by setting background points maximum to 10,000 (Merow et al., 2013). The model parameters were set to 5 replicates and results were obtained from the average of all replicates of each model.

Results

Microscopic imaging at 100x showed that *B. papyrifera* pollen is round to oval in shape, with three scar–like structures on the outer surface of the exine layer protecting the intine layer and the pollen. Pollen from different regions had no significant morphological differences (Fig. 1) but had variations in their FTIR spectra. Pollen FTIR analysis showed variations in the protein region amide-II and amide–I, and lipid region. The environmental conditions of the three regions sampled varied in terms of mean annual temperature and mean annual precipitation (S1 Fig., S2 Fig.). Analysis of the data showed that there is a gradual increase in mean annual temperature, and a gradual decrease mean annual precipitation across

all regions. There is an increase in spring maximum pollen counts in a single day. The LC-MS/MS analysis of summer pollen 2020 showed 33 different organic compounds. These compounds were from six organic groups where alkaloids were abundant. Terpenes, alkanes, and straight-chain fatty acids (SCFA) were at the lowest concentration in the pollen samples. Four lipid compounds (succinic acid, adipic acid, pimelic acid, and sebacic acid) which have been reported to have a role in pollen allergies of some subjects (Bashir et al., 2013; Caimmi et al., 2008).

The R1 pollen (Fig. 1A and D) have a rough exine shown as a dotted appearance, while R2 and R3 pollen (Fig. 1B, C, E and F) have a smooth exine. R1 has slight high mean annual temperature as compare to R2 and R3. Exine lengths of three pollens were calculated through ImageJ software for each location and average length was calculated. Exine length average values are given in Table 1.

Table 1
Average exine length calculation through ImageJ

Image name	Location and Time	Average µm
A	Spring 2020 Peshawar	22.67
B	Spring 2020 Islamabad	23.05
C	Spring 2020 Kotli	24.13
D	Spring 2021 Peshawar	22.87
E	Spring 2021 Islamabad	22.26
F	Spring 2021 Kotli	24.43

Fourier Transform Infrared Spectroscopy (FTIR) of Pollen

FTIR analysis of pollen (Fig. 2A) collected from R1, R2 and R3 in the spring 2020 using a spectral wavelength of 500–3000 nm showed spectral regions of the protein (1700–1500 cm^{-1}), and lipid (2900–2700 cm^{-1}) which were analyzed. The region between 1750 cm^{-1} to 2750 cm^{-1} exhibited more differences in comparison to other spectral regions. Figure 2B shows FTIR spectra of pollen samples collected from R1, R2, and R3 in spring 2020 and 2021. The spectra for R1, R2 and R3 pollen varies for percent transmittance values. Spring 2020 pollen have greater differences in pollen spectra as compared to spring 2021 pollen. The spectral differences associate with chemical bonds for proteins and lipids are listed in Table 2.

Table 2
Spectral zone, functional group frequencies, and associated chemical bonds

Spectral zone	Peak frequency cm^{-1}	Chemical bonds
Lipids	2930	CH_3 stretching (lipids)
	2850	CH_2 stretching (lipids)
Amide I	1620 β-sheet	NH_2 bending
1700 – 1600 cm^{-1}	1650 α-helix	N-O stretch
Amide II	1670 β-turn	
1600 – 1500 cm^{-1}	1550	

The table shows spectral zones of lipids and proteins along with peak frequencies and chemical bonds (J. Depciuch et al., 2017).

B. papyrifera pollen collected at natural environmental conditions analysed by FTIR showed differences in protein region for R1, R2 and R3, and between spring 2020 and spring 2021 pollen (Fig. 3A and Fig. 3B). Spectral difference in peak heights occur in Amide-II and Amide-I functional groups (1500–1700 wavelength). Amide-II region spectral peaks differ for all sites pollen at 1550 cm^{-1} wavelength in transmittance for N-O stretch. Similarly, the spectral peaks differ at 1620 cm^{-1} β-sheet, 1650 α-helix and 1670 β-turn of NH_2 functional group in 2020 and 2021. R2 and R3 have sharp peaks N-O stretch at 1550 cm^{-1}, 1620 cm^{-1} β-sheet, 1650 α-helix and 1670 β-turn of (NH_2 functional group) in 2021 and 2020. The peaks for these wavelengths differ between spring 2021 and spring 2020 pollens for all sites.

Lipid region has variation in peak intensities in 2020 for CH_2 and CH_3 functional groups at 2850 cm^{-1} and 2930 cm^{-1} for R1, R2 and R3 (Fig. 4A and Fig. 4B). The pollens of same region have lost peak intensities in 2021. These variations in spectral peaks reflect differences in weather conditions impact on pollen structures.

Light Chromatography-Mass Spectrometry (LCMS) Analysis

LCMS analysis of *B. papyrifera*-pollen run time is 17 minutes (see Fig. 5). LCMS analysis identified large number of different compounds given in S1 Table. These compounds categorized in seven groups such as alkaloids, carboxylic acids, alkanes, straight-chain fatty acids (SCFA), terpenes, unsaturated fatty acids (USFA) and other lipids as shown in Fig. 6. Alkaloids occur in high numbers (12) followed by other lipids (9) and carboxylic acids (5). Alkanes, SCFA, and terpenes are found very little in quantity. There was only 1 SCFA ($C_{30}H_{52}O_2$), 1 alkene ($C_{21}H_{23}O_3P$), and 1 terpene ($C_{21}H_{26}N_2O_5$). Saturated fatty acids identified in this study include – Succinic acid, hexyl 2-phenylethyl ester ($C_{18}H_{26}O_4$), Adipic acid, di (2-phenylethyl) ester ($C_{22}H_{26}O_4$), Pimelic acid, di(phenethyl) ester ($C_{23}H_{28}O_4$), and Sebacic acid, 2-methylbenzyl undecyl ester ($C_{29}H_{48}O_4$) in the target pollen.

In vitro IgE binding to B. papyrifera pollen proteins

Selected serum 1:10 diluted samples in non-fat dry milk were cross reacted with *B. papyrifera* pollen protein extracts in 1X PBS and 1:10 (1X PBS) diluted through dot blots. Positive serum samples (Fig. 7) were shortlisted for western blotting to identify allergens in the pollen protein extracts.

Allergenic proteins present in the selected sera were determined through SDS gel electrophoresis and western blotting. Western blotting identified four protein bands in lane 1 and lane 2 (see Fig. 8).The band sizes 40 kDa, 33 kDa, 15 kDa and 10 kDa were confirmed by comparison of the western blot with the stained gel on the stage of the imager after western blot visualization. Three protein bands 40 kDa, 33 kDa and 10 kDa were previously identified while 15 kDa protein band is not reported in any literature so far.

Precipitation, temperature and pollen count

The three decades data analysis (1991–2020) for R1 and R2 and a single decade data (2010–2020) available from PMD showed decrease in mean annual precipitation and increase in mean annual temperature during this period for the selected three regions (see S1 Fig. and S2 Fig.). The trend line for this period shows about 13 mm mean annual temperature decrease for R1 while the trend line for R2 and R3 shows few mm mean annual temperature decrease. Similarly, the temperature change trend line for all the three regions show an increase in temperature for the mentioned period. About 0.45°C increase in mean annual temperature has occurred for R1. About 0.2°C increase in mean annual temperature has occurred in R2 and R3. Analysis of spring maximum single day pollen count in 1 cubic meter in R2 has found an increase in pollen count production during 2003–2022 (see S3 Fig.). Maximum single day pollen count was 38946 in 2003 that has reached to highest 49465 in 2022.

Model performance of the Maxent model

The area under curve (AUC) is a built-in statistical package in MaxEnt that evaluates model performance based on the presence of records data only (van Proosdij et al., 2016). The AUC test exhibited 0.968, 0.99, 0.99, 0.938, 0.962, 0.987, 0.959, and 0.881 for training data of all models that showed excellent performance of the model in predicting the potential distribution of *B. papyrifera* in Asia in the years 2050 and 2070 under RCP 4.5 and RCP 8.5 (Fig. 9).

Bioclimatic variables BIO1 (mean annual temperature), BIO10 (mean temperature of warmest quarter), and BIO11 (mean temperature of coldest quarter) have significant contribution in the model analysis presented in Fig. 10. Permutation importance of these three variables was highest of all other variables that predict change in the values of these variables in future will add to the invasion of the plant growth. MaxEnt modeling through ACCESS10 for climate change scenario RCP 4.5 and RCP 8.5 shows a perspective increase in the occurrence of the *B. papyrifera* in Asia. The increase occurs due to increase in mean annual temperature, **AC4.5bi50** showed a greater increase in the possible invasion of the tree in Saudi Arabia, Iraq, Jordan, Syria, Turkey, Iran, Afghanistan, Turkmenistan, Uzbekistan, Afghanistan, Pakistan, India, and Nepal; and a slight increase in China, Hong Kong, and Myanmar. Models **AC4.5bi70**

and **AC8.5bi50** having almost similar temperature conditions showed invasion in almost similar regions of Asia. *B. papyrifera* will possibly invade regions of Saudi Arabia, Iran, Pakistan, India, Afghanistan, China, Nepal, Hong Kong, and Japan. Prospective invasion of *B. papyrifera* in **AC8.5bi50** model is similar to AC4.5bi50 but the area covered in this model is greater and the intensity of plant growth is also greater. Both RCP 4.5 and 8.5 scenarios in the years 2050 and 2070 show invasion of the tree into uninvaded regions in the future. The future invasion occurs in Saudi Arabia, Iraq, Turkey, Iran, Afghanistan, Turkmenistan, Uzbekistan, Afghanistan, Pakistan, India, Nepal, China, Hong Kong, Japan, and Myanmar according to RCP4.5 in the year 2070. RCP 4.5 in the year 2050 and RCP 8.5 in the years 2050 and 2070.

Bioclimatic variables BIO1 (mean annual temperature), BIO10 (mean temperature of warmest quarter), and BIO11 (mean temperature of coldest quarter) contributed to the model future assessment analysis shown in Fig. 7. The model has assessed that change in the values of these three variables in the future will add to the invasion of the plant growth to new locations in Asia. MaxEnt modeling through CCSM4 for climate change scenario RCP 4.5 and RCP 8.5 shows the prospective increase in the occurrence of the *B. papyrifera* tree. **CC4.5bi50** shows the possible invasion of the tree similar to **AC4.5bi50** and **AC4.5bi70** with a slight difference in the invasion intensity. However, **CC8.5bi50** showed a prospective invasion of the tree in almost half of Asia in the year 2050 while the tree invasion will continue in almost the whole of Asia by the year 2070 according to **CC8.5bi70.** Both RCP 4.5 and 8.5 scenarios in the years 2050 and 2070 show the greater invasion of the tree into uninvaded regions in the years 2050 and 2070. Both models (Access 1.0 and CCSM4) predict invasion of B. papyrifera into new locations in Asia in the years 2050 and 2070 climate change scenarios RCP 4.5 and RCP 8.5. However, CCSM4 model predicts high invasion of the specie as compared to ACCESS1.0 model in 2050 and 2070 under RCP 4.5 and RCP 8.5.

Discussion

The *B. papyrifera* distribution, habitat, plant size, growth rate, and uses have been well described (Whistler & Elevitch, 2006). Only male clone introduction of the species to Pacific islands stopped its invasion into other regions due to the absence of seeds. The pollen allergenicity of the plant was explained and 10 kDa allergen was identified through IgE testing, but not sequenced (Micheal et al., 2013). Later on 33 kDa and 40 kDa pollen allergens in *B. Papyrifera* were identified through IgE immunoblot analysis but not sequenced (Aslam et al., 2015). The impacts of weather patterns on *B. papyrifera* pollen concentrations were investigated (Cheema et al., 2016) and a strong correlation was observed between temperature and pollen count. Increase in temperature above 25°C supports increase in pollen count during pollination. The current research aimed at investigating climate change factors' impact on *B. papyrifera*-pollen composition, pollen allergenicity, estimation of future plant distribution in response to climate change, and metabolome analysis through LC-MS/MS. Environmental factors have shown a significant impact on the pollen's biochemical composition. In our investigations the FTIR analysis exhibited spectra between 4000 cm^{-1}–400 cm^{-1} that covered both fingerprint (400 cm^{-1}–1500 cm^{-1}) region and functional group region (4000 cm^{-1}–1000 cm^{-1}). Infrared light transmitted through pollen obtained spectra that analysed all compounds present in the pollen (see Fig. 2–4) and differences in pollen are evident from differences

in the spectral peaks. Spectra for the same plant species distribution in different climatic regions showed variations in the peak height and peak area for protein Amide-II and Amide-I regions. Similarly, variations in spectral peaks occurred for the same species of pollen collected in spring 2020 and spring 2021 in the same climatic region. The studies suggest that the pollen samples may possess quantitative differences in their biochemical composition due to differences in mean annual temperature. Pollen structure comprises of lipids, carbohydrates, and proteins (Blackmore et al., 2007; Costa et al., 2015; Jia et al., 2015; Pérez-Pérez et al., 2019; Quilichini et al., 2015), and change in FTIR spectra peaks for protein and lipid region can be due to changes in the functional groups of biomolecules making pollen proteins and lipids (Fig. 3 and Fig. 4). The *B. papyrifera*-pollen FTIR analysis, for lipids and proteins functional groups showed inter–regional differences in pollen grains (Fig. 2). CH_2 and CH_3 stretching of lipids at 2850 cm^{-1} and 2930 cm^{-1} differ in peak heights for pollen collected in spring 2020 in R1, R2 and R3. These regions have variations in temperature and precipitation that may have a possible effect on the pollen biochemical composition. R1 has different environmental conditions in comparison to R2 and R3, and the respective pollen spectra varied in the protein region (1500 cm^{-1}–1700 cm^{-1}). The protein region comprises Amide I (1600 cm^{-1}-1700 cm^{-1}), and Amide II (1700 cm^{-1}–1600 cm^{-1}). For Amide II, the peak area at 1550 cm^{-1} for the functional group [Nitroso (NO) stretch] varies. Amide I region peaks area at 1620 cm^{-1}, 1650 cm^{-1}, and 1670 cm^{-1} for β-sheet, α-helix, and β-turn differ from one another. Similarly, the NO-stretch peak area for spring 2021 for all three pollen samples is different. Peaks area in the Amide I region for β-sheet, α-Helix, and β-turn are similar for R2 and R3, and vary for R1 (Table 1, 3). These results of FTIR are in good agreement with the previous findings, which showed temperature and precipitation effects on pollen chemical composition and viability of *Syringa vulgaris* L. (Kenđel & Zimmermann, 2020). They found spectral differences in pollen of different species. Our findings show spectral differences in *B. papyrifera* pollen (protein region) collected from different locations having varied temperature and precipitation conditions. Moreover, the present study is the first to exploit metabolome investigations and allergy potency of *B. papyrifera* pollen in response to climate change. Previous investigations have demonstrated that a temperature difference of 4°C at a 200 m elevation gradient has a negative effect on *Pinus edulis* pollen germination, reproduction, and viability (Flores-Rentería et al., 2018; Pacini & Dolferus, 2019). Periods of high-temperature cause bursting of the tapetum layer resulting in pollen sterility (Giorno et al., 2013). The current research has correlated different elevations and temperature condition effects on pollens' biochemical composition through FTIR analysis, which showed significant differences in pollen collected at different elevations and different temperature and precipitation conditions. Pollen tolerance to variation in temperature and elevation has been found to affect pollen viability negatively (Flores-Rentería et al., 2018). Climatic effects on pollen are evident from pollen light microscopy images (Fig. 1), and FTIR spectra. Spring 2020 pollen spectra (Fig. 2A) differ from spring 2021 pollen spectra (Fig. 2B). The protein region of Amide-I (β-sheet, α-helix, and β-turn) has variation in the functional group of NH_2 bending, and the Amide-II region has a difference in the functional group of NO–stretch. Similar findings of heat stress effects have been studied in wheat pollen, where heat stress altered pollen lipid composition by remodeling extraplastidic phospholipids. Heat stress decreased the quantity of more unsaturated extraplastidic phospholipids, and increased the quantity of

less unsaturated extraplastidic phospholipids (Narayanan et al., 2018). Moreover, variation in environmental conditions has been found to change lipids, carbohydrates, and protein expression in 813 pollen specimens from 300 distinct plant species grown in 5 different pollen seasons (Zimmermann & Kohler, 2014). Similarly, the current study of pollen protein analysis through FTIR showed inter–regional differences. Amide-II peak of NO–stretch at 1550 cm^{-1} for R2 differs between spring 2020 and spring 2021 pollens. Amide-I peak for β-sheets is at 1620 cm^{-1} in spring 2020 pollen while the same peak for spring 2021 samples is less intense and at 1618 cm^{-1}. α-helix peak is less intense and overlaps between R1 and R2 in spring 2020 pollen at 1650 cm^{-1} while the same peak for R3 is intense and unique. However, in spring 2021 the same peak is intense for R2and R3 while for R1 the peak intensity has lowered. β-turn of R1 peak at 1670 cm^{-1} in spring 2020 and spring 2021 pollen differs from R2 and R3. These inter–regional differences in the protein region of FTIR peaks are due to variations in temperature and precipitation conditions (S1 Fig., S2 Fig., and Fig. 3). Similar findings were made for hazel interregional pollen comparison through FTIR spectroscopy. Such variations in pollen biochemical structure are adaptive to weather differences (J. Depciuch et al., 2017). Comparably, FTIR spectroscopy has identified adaptive variations in the chemical composition of proteins, lipids, and carbohydrates in pollen of *Poa alpine, Anthoxanthum odoratum*, and *Festuca ovina* has grown in different geographic and climatic conditions (Zimmermann et al., 2017). Those investigations supported the idea that increases in temperature and differences in elevation can alter pollen chemical composition. The mean annual temperature of R1 is higher than R2 and R1, and the mean annual precipitation of R1 is low than R2 and R3. Similarly, spring 2021 pollen specimen analysis showed variation in protein regions in the FTIR spectra. R1 has extreme climatic conditions (high temperature and less precipitation) in comparison to R2 and R3 having moderate variations in weather conditions. The spectra analyzed for the three regions show elevated peaks and intense transmission for R1 as compared to R2 and R3. This enhancement in the spectra for R1 can be correlated to the weather conditions (S1 Fig.). The FTIR peaks in the region of proteins and lipids functional groups collected during different seasons and from different regions varied in terms of infrared light transmission and peak area (Fig. 3, Fig. 4). Elevated temperature in R1 as compared to R2 and R3 may have a possible effect on *B. papyrifera*-pollen composition. The high–temperature stress role in association with in-vitro pollen germination and pollen tube growth in *Pisum sativum* L. modification has been verified (Jiang et al., 2017).

The difference in temperature, precipitation, and geographic location is correlated with differences in the spectral region of *B. papyrifera* while variation in temperature and precipitation act as stress that activates an oxidative stress response in plants that alter pollen metabolism and development. High–temperature stress to pollen yields an increase in pollen proteins while low–temperature stress causes enhancement of pollen lipids and carbohydrates (Jiang et al., 2019; Zimmermann et al., 2017). The spectral differences in pollen have been reflected for *B. papyrifera* pollen collected in spring 2020 from different regions in spring 2020 and 2021 having variance in average temperature and average precipitation (Fig. 2). An increase in temperature and decrease in precipitation has been found to affect pollen weight, protein content, and allergen contents (Jung et al., 2021). In a recent study, on honeybee pollen PCA analysis has shown significant differences in pollen biochemical composition (Zeghoud et al.,

2021), which further strengthens the findings of our research that pollen chemical composition varies with change in elevation and temperature.

The *B. papyrifera* produces allergenic pollen that causes hypersensitivity in human partly because of small size (12–17 µm) and are capable to pass through the human nasal cavity and reach deep into the lungs. Two allergens in *B. papyrifera* pollen have been identified (Aslam et al., 2015). Our investigations on *B. papyrifera* pollens' metabolome analysis through LC-MS/MS have found the presence of succinic acid, hexyl 2-phenylethyl ester ($C_{18}H_{26}O_4$), adipic acid, di (2-phenylethyl) ester ($C_{22}H_{26}O_4$), pimelic acid, di (phenethyl) ester ($C_{23}H_{28}O_4$), and sebacic acid, 2-methylbenzyl undecyl ester ($C_{29}H_{48}O_4$). Bashir et al. (2013) have found these compounds' role in activating cytokine expression of DC/NKT cells and marked these as potential biomarkers. The pollen contains 4 saturated fatty acids that induce Thelper2 (TH2) cells associated Interleukine-13 (IL13) which are involved in nasal allergies in humans (Bashir et al., 2013). Exposure of epithelial layers of the deep nasal cavity to such small pollen that possess both allergens and allergenic metabolites may be involved in the incitation of the human immune system. We assume that this can be the possible reason for the high pollen allergies incidences in district C and surrounding areas during the flowering season, where the daily pollen count in the air reaches 45000 grains/m. Climate factors affects pollen composition and plant growth distribution.

This study reports 4 allergens in *B. papyrifera* pollen. Earlier 3 allergens 33 kDa, 40 kDa and 10 kDa were reported in *B. papyrifera* pollen through ELISA and blotting studies (Aslam et al., 2015; Micheal et al., 2013). This study confirms the presence of 33 kDa, 40 kDa and 10 kDa allergens in the *B. papyrifera* pollen, and finds one novel allergen of about 15 kDa through western blotting. Earlier studies records of moraceae family in "Allergenonline.org and Allergen.org" show 4 allergens. Out of these four, Mor n 3 (non-specific lipid transfer protein) and two other 18 kDa unassigned, are food allergens. Mor a 2 (cobalamin-independent methionine synthase) is the only registered airway allergens of 84 kDa in allergen.org. This study found one novel and verified three previously identified airway allergens in *B. papyrifera* a member of moraceae family. None of the four allergens identified in this study are registered in Allergenonline.org and Allergen.org so far. The 15 kDa lower molecular weight airway allergens found in this study is not reported in any literature so far. All these four allergens add an explanation to increasing airway allergies caused in spring and summer during blooming of *B. papyrifera* in Pakistan.

Like other plant species *B. papyrifera* is also prone to climate change effects. MaxEnt modeling estimates a moderate increase in global temperature and carbon availability in the atmosphere according to representative concentration pathway (RCP) 4.5 (Thomson et al., 2011) which supports the invasion of *B. papyrifera* into new regions of Asia (Fig. 9). Similarly, an extreme increase in global temperature and carbon emissions according to representative concentration pathway (RCP) 8.5 (Riahi et al., 2011) assessed through MaxEnt modeling suggests the invasion of *B. papyrifera* into uninvaded regions of Asia (Fig. 10). Both models ACCESS1.0 and CCSM4 assessed through Maxent have estimated expansion of the allergenic specie into new locations. Further, analysis of bioclimatic variables percent contribution and permutation to the two models assessed (mean annual temperature (BIO1), mean temperature of warmest quarter (BIO10), and mean temperature of coldest quarter (BIO11) role in *B. papyrifera* invasion.

Increase in BIO1, BIO10 and BIO11 values in future due to climate change contribute to the model output. Increase in these variables values in future occur due to increase in carbon emissions (Valone, 2021). Both temperature rise and greater availability of carbondioxide in the atmosphere support photosynthesis process making suitablity of *B. papyrifera* growth in new regions. Invasion of the allergenic plant species into new regions can increase allergies burden in these regions. Allergenic availability in the uninvaded regions will expose the susceptible human population to the allergenic pollen that may invoke immune reactions in them. This aspect of allergies bundle increase has been estimated and ragweed pollen allergy will be a common health problem in Europe in the future due to ragweed invasion into new areas (Lake et al., 2018).

The current study has found a decrease in precipitation and an increase in temperature in all the three regions since 1991–2022 according to the data available from PMD. The study does not determine factors for this change in the climatic factors but this change can be due to anthropogenic actions. Maximum spring pollen count increase in a single day in one cubic meter has occurred in R2 in the mentioned period (2003–2022) from 38946 pollen grains/m^3 to 49465 pollen grains/m^3 that can be correlated to mean annual temperature increase in the region over time. Similar, findings were made on a historical temperature increase and pollen count increase data correlation study in Madrid Spain. The study has been found that an increase in 1.3°C temperature, has increased *Cupressaceae, Platanus*, and *Quercus* pollen by approximately 3,000, 9,000, and 5,000 pollen grains/m3, respectively (Subiza et al., 2019). The *B. papyrifera* produces greater quantities of pollen during the flowering season in comparison to other plant species. Therefore, expansion in plant distribution and increase in temperature may increase *B. papyrifera* allergenic pollen production. The recent heatwave of 2022 badly affected the population in South Asia where the earth's surface temperature reached a record 50°C in parts of Pakistan and India in the month of April. An increase in the earth's surface temperature can deteriorate pollen composition and pollen quantity subjecting a greater population in the region to a higher risk of getting pollen allergies. High human population growth in Asia especially in South Asia, and socio-economic development may intensify global warming and climate change in the present and future (Pawankar et al., 2020). These factors increase the temperature of cold weather regions making them suitable for the *B. papyrifera* growth. The expansion of the allergenic tree in new regions in the future may cause an increase in pollen allergies episodes in Asia due to the combined effect of *B. papyrifera* invasion and the expected increase in pollen production in the future.

Conclusion

Our state-of-the-art investigations have found a novel airway allergen (about 15 kDa) in *B. papyrifera* pollen through western blotting and verified presence of three other allergens reported earlier. So far, none of these four airway allergens are registered in Allergenonline.org and Allergen.org. The unique findings of this study demonstrate that climatic factors like temperature and precipitation have a significant effect on *B. papyrifera* pollen production, morphology and pollen chemical composition (proteins and lipids contents). An increase in temperature, decrease in precipitation, and difference in elevation yield variation

in *B. papyrifera* pollen grains' biochemical structure. The effects of climate factors on the pollen morphology and chemical composition are based on geographic locality. *B. papyrifera* MaxEnt modeling has estimated invasion of the plants in new locations in Asia invading 20 countries in the years 2050 and 2070. Among 33 different organic compounds, identified by LCMS analysis, 4 saturated fatty acid compounds have a possible role in the elicitation of cytokine expression of DC/NKT cells in the human immune system in the form of allergies. Therefore, it is predicted that climate change effects on *B. papyrifera* pollen composition and growth distribution, may enhance allergic diseases in Asia. The findings of this study are novel for researchers and policy makers, which may provide a baseline model system for predicting variation in pollen structure and associated allergies for other species in response to climate shift.

Declarations

Conflict of interest

The author declares that there is no conflict of interest.

Acknowledgments

We are thankful to the Higher Education Commission (HEC) Pakistan for providing financial support to conduct this study under the umbrella of HEC-NRPU Project No. 8231 titled "Strategic development of baseline protocols to predict climate change impacts on plants and prevalence of associated allergies in Pakistan". We are also thankful to Climate Data Processing Centre, Pakistan Meteorological Department Pakistan for providing precipitation and temperature data.

Authors Contribution

MH performed the experiment, compiled the data and wrote the manuscript. SN helped in project execution, data compilation and analysis and wrote the manuscript. ZA conceptualized the idea, designed the experimental strategies, reviewed the manuscript and supervised the whole project. RG helped with experimental design, co-supervised the work, reviewed the manuscript, and improved the English language of the manuscript.

References

1. Ajani, A., & van der Geest, K. (2021). Climate change in rural Pakistan: evidence and experiences from a people-centered perspective. Sustainability Science, *16*(6), 1999–2011. https://doi.org/10.1007/s11625-021-01036-4
2. Anderegg, W. R. L., Abatzoglou, J. T., Anderegg, L. D. L., Bielory, L., Kinney, P. L., & Ziska, L. (2021). Anthropogenic climate change is worsening North American pollen seasons. Proceedings of the National Academy of Sciences of the United States of America, *118*(7), 1–6. https://doi.org/10.1073/pnas.2013284118

3. Aslam, M., Khalid, T., Gull, I., Abbas, Z., & Athar, M. A. (2015). Original Research Identification of Major Allergens of Paper Mulberry (Broussonetia Papyriferra) Pollens and Purification of Novel 40 kDa Allergen Protein. In *Current Allergy & Clinical Immunology* (Vol. 28, Issue 1).
4. Bashir, M. E. H., Lui, J. H., Palnivelu, R., Naclerio, R. M., & Preuss, D. (2013). Pollen Lipidomics: Lipid Profiling Exposes a Notable Diversity in 22 Allergenic Pollen and Potential Biomarkers of the Allergic Immune Response. PLoS ONE, *8*(2). https://doi.org/10.1371/journal.pone.0057566
5. Blackmore, S., Wortley, A. H., Skvarla, J. J., & Rowley, J. R. (2007). Pollen wall development in flowering plants: Tansley review. New Phytologist, *174*(3), 483–498. https://doi.org/10.1111/j.1469-8137.2007.02060.x
6. Caimmi, S., Caimmi, D., Bousquet, P. J., & Demoly, P. (2008). Succinate as opposed to glucocorticoid itself allergy. Allergy: European Journal of Allergy and Clinical Immunology, *63*(12), 1641–1643. https://doi.org/10.1111/j.1398-9995.2008.01894.x
7. Cheema, S. B., Afzal, M., & Anjum, M. A. (2016). *Impacts of Weather Pattern on Pollen Concentration in Islamabad*. http://www.pmd.gov.pk/Pollen_Report_2016.pdf
8. Costa, M. L., Sobral, R., Costa, M. M. R., Amorim, M. I., & Coimbra, S. (2015). Evaluation of the presence of arabinogalactan proteins and pectins during Quercus suber male gametogenesis. Annals of Botany, *115*(1), 81–92. https://doi.org/10.1093/aob/mcu223
9. Dahl, Å. (2018). Pollen Lipids Can Play a Role in Allergic Airway Inflammation. Frontiers in Immunology, *9*(December), 2816. https://doi.org/10.3389/fimmu.2018.02816
10. Damialis, A., Gilles, S., Sofiev, M., Sofieva, V., & Kolek, F. (2021). *Higher airborne pollen concentrations correlated with increased SARS-CoV-2 infection rates, as evidenced from 31 countries across the globe*. *118*(12), 1–10. https://doi.org/10.1073/pnas.2019034118/-/DCSupplemental.Published
11. Damialis, A., Traidl-Hoffmann, C., & Treudler, R. (2019). Climate Change and Pollen Allergies. In *Biodiversity and Health in the Face of Climate Change* (pp. 47–66). https://doi.org/10.1007/978-3-030-02318-8_3
12. de Weger, L. A., Pashley, C. H., Šikoparija, B., Skjøth, C. A., Kasprzyk, I., Grewling, Ł., Thibaudon, M., Magyar, D., & Smith, M. (2016). The long distance transport of airborne Ambrosia pollen to the UK and the Netherlands from Central and south Europe. International Journal of Biometeorology, *60*(12), 1829–1839. https://doi.org/10.1007/s00484-016-1170-7
13. Depciuch, J., Kasprzyk, I., Sadik, O., & Parlińska-Wojtan, M. (2017). FTIR analysis of molecular composition changes in hazel pollen from unpolluted and urbanized areas. Aerobiologia, *33*(1), 1–12. https://doi.org/10.1007/s10453-016-9445-3
14. Depciuch, Joanna, Kasprzyk, I., & Drzymała, E. (2018). Identification of birch pollen species using FTIR spectroscopy. Aerobiologia, *34*(4), 525–538. https://doi.org/10.1007/s10453-018-9528-4
15. Flores-Rentería, L., Whipple, A. V., Benally, G. J., Patterson, A., Canyon, B., & Gehring, C. A. (2018). Higher temperature at lower elevation sites fails to promote acclimation or adaptation to heat stress during pollen germination. Frontiers in Plant Science, *9*(April), 1–14. https://doi.org/10.3389/fpls.2018.00536

16. Fragallah, S. A. D. A., Wang, P., Li, N., Chen, Y., & Lin, S. (2018). Metabolomic Analysis of Pollen Grains with Different Germination Abilities from Two Clones of Chinese Fir (Cunninghamia lanceolata (Lamb) Hook). Molecules, *23*(12). https://doi.org/10.3390/molecules23123162
17. Giorno, F., Wolters-Arts, M., Mariani, C., & Rieu, I. (2013). Ensuring reproduction at high temperatures: The heat stress response during anther and pollen development. Plants, *2*(3), 489–506. https://doi.org/10.3390/plants2030489
18. Hijmans, R. J., Cameron, S. E., Parra, J. L., Jones, P. G., & Jarvis, A. (2005). Very high resolution interpolated climate surfaces for global land areas. International Journal of Climatology, *25*(15), 1965–1978. https://doi.org/10.1002/joc.1276
19. Ischebeck, T. (2016). Lipids in pollen — They are different. Biochimica et Biophysica Acta - Molecular and Cell Biology of Lipids, *1861*(9), 1315–1328. https://doi.org/10.1016/j.bbalip.2016.03.023
20. Jia, Q. S., Zhu, J., Xu, X. F., Lou, Y., Zhang, Z. L., Zhang, Z. P., & Yang, Z. N. (2015). Arabidopsis AT-hook protein TEK positively regulates the expression of Arabinogalactan proteins for nexine formation. Molecular Plant, *8*(2), 251–260. https://doi.org/10.1016/j.molp.2014.10.001
21. Jiang, Y., Bueckert, R. A., Warkentin, T. D., & Davis, A. R. (2017). High temperature effects on in vitro pollen germination and seed set in field pea. Canadian Journal of Plant Science, *98*(1), 71–80. https://doi.org/10.1139/cjps-2017-0073
22. Jiang, Y., Lahlali, R., Karunakaran, C., Warkentin, T. D., Davis, A. R., & Bueckert, R. A. (2019). Pollen, ovules, and pollination in pea: Success, failure, and resilience in heat. Plant Cell and Environment, *42*(1), 354–372. https://doi.org/10.1111/pce.13427
23. Jung, S., Estrella, N., Pfaffl, M. W., Hartmann, S., Ewald, F., & Menzel, A. (2021). Impact of elevated air temperature and drought on pollen characteristics of major agricultural grass species. PLoS ONE, *16*(3 March), 1–19. https://doi.org/10.1371/journal.pone.0248759
24. Kang, K. Bin, Woo, S., Ernst, M., van der Hooft, J. J. J., Nothias, L. F., da Silva, R. R., Dorrestein, P. C., Sung, S. H., & Lee, M. (2020). Assessing specialized metabolite diversity of Alnus species by a digitized LC–MS/MS data analysis workflow. *Phytochemistry*, *173*. https://doi.org/10.1016/j.phytochem.2020.112292
25. Kenđel, A., & Zimmermann, B. (2020). Chemical Analysis of Pollen by FT-Raman and FTIR Spectroscopies. Frontiers in Plant Science, *11*(March), 1–19. https://doi.org/10.3389/fpls.2020.00352
26. Lake, I. R., Jones, N. R., Agnew, M., Goodess, C. M., Giorgi, F., Hamaoui-Laguel, L., Semenov, M. A., Solmon, F., Storkey, J., Vautard, R., & Epstein, M. M. (2018). Erratum: "Climate Change and Future Pollen Allergy in Europe." Environmental Health Perspectives, *126*(7), 079002. https://doi.org/10.1289/EHP2073
27. Merow, C., Smith, M. J., & Silander, J. A. (2013). A practical guide to MaxEnt for modeling species' distributions: What it does, and why inputs and settings matter. Ecography, *36*(10), 1058–1069. https://doi.org/10.1111/j.1600-0587.2013.07872.x

28. Micheal, S., Wangorsch, A., Wolfheimer, S., Foetisch, K., Minhas, K., Scheurer, S., & Ahmed, A. (2013). Immunoglobulin E reactivity and allergenic potency of Morus papyrifera (paper mulberry) Pollen. Journal of Investigational Allergology and Clinical Immunology, *23*(3), 168–175.
29. Mittler, R. (2017). ROS Are Good. Trends in Plant Science, *22*(1), 11–19. https://doi.org/10.1016/j.tplants.2016.08.002
30. Mohanty, R. P., Buchheim, M. A., Anderson, J., & Levetin, E. (2017). Molecular analysis confirms the long-distance transport of Juniperus ashei pollen. PLoS ONE, *12*(3), 1–13. https://doi.org/10.1371/journal.pone.0173465
31. Narayanan, S., Prasad, P. V. V., & Welti, R. (2018). Alterations in wheat pollen lipidome during high day and night temperature stress. Plant Cell and Environment, *41*(8), 1749–1761. https://doi.org/10.1111/pce.13156
32. Pacini, E., & Dolferus, R. (2019). Pollen developmental arrest: Maintaining pollen fertility in a world with a changing climate. Frontiers in Plant Science, *10*(May), 1–15. https://doi.org/10.3389/fpls.2019.00679
33. Papia, F., Incorvaia, C., Genovese, L., Gangemi, S., & Minciullo, P. L. (2020). Allergic reactions to genus Morus plants: a review. *Clinical and Molecular Allergy*, *October 2018*, 1–5. https://doi.org/10.1186/s12948-020-00116-7
34. Parrotta, L., Faleri, C., Cresti, M., & Cai, G. (2016). Heat stress affects the cytoskeleton and the delivery of sucrose synthase in tobacco pollen tubes. Planta, *243*(1), 43–63. https://doi.org/10.1007/s00425-015-2394-1
35. Pawankar, R., Wang, J.-Y., Wang, I.-J., Thien, F., Chang, Y.-S., Latiff, A. H. A., Fujisawa, T., Zhang, L., Thong, B. Y.-H., Chatchatee, P., Leung, T. F., Kamchaisatian, W., Rengganis, I., Yoon, H. J., Munkhbayarlakh, S., Recto, M. T., Neo, A. G. E., Le Pham, D., Lan, L. T. T., … Oh, J. W. (2020). Asia Pacific Association of Allergy Asthma and Clinical Immunology White Paper 2020 on climate change, air pollution, and biodiversity in Asia-Pacific and impact on allergic diseases. Asia Pacific Allergy, *10*(1), 1–19. https://doi.org/10.5415/apallergy.2020.10.e11
36. Pérez-Pérez, Y., Carneros, E., Berenguer, E., Solís, M. T., Bárány, I., Pintos, B., Gómez-Garay, A., Risueño, M. C., & Testillano, P. S. (2019). Pectin de-methylesterification and AGP increase promote cell wall remodeling and are required during somatic embryogenesis of quercus suber. Frontiers in Plant Science, *9*(January), 1–17. https://doi.org/10.3389/fpls.2018.01915
37. Phillips, S. (2008). A Brief Tutorial on Maxent. AT&T Research. AT&T Research, 1–38.
38. Quilichini, T. D., Grienenberger, E., & Douglas, C. J. (2015). The biosynthesis, composition and assembly of the outer pollen wall: A tough case to crack. Phytochemistry, *113*, 170–182. https://doi.org/10.1016/j.phytochem.2014.05.002
39. Ramadan, S., Marsh, J., El-Sherbeny, G. A., El-Halawany, E. S. F., Luan, F., Baumert, J. L., Johnson, P., Osman, Y., & Goodman, R. E. (2021). Purification of soybean cupins and comparison of IgE binding with peanut allergens in a population of allergic subjects. *Food and Chemical Toxicology*, *147*(November 2020), 111866. https://doi.org/10.1016/j.fct.2020.111866

40. Riahi, K., Rao, S., Krey, V., Cho, C., Chirkov, V., Fischer, G., Kindermann, G., Nakicenovic, N., & Rafaj, P. (2011). RCP 8.5-A scenario of comparatively high greenhouse gas emissions. Climatic Change, *109*(1), 33–57. https://doi.org/10.1007/s10584-011-0149-y
41. Saleem, F., Zeng, X., Hina, S., & Omer, A. (2021). Regional changes in extreme temperature records over Pakistan and their relation to Pacific variability. Atmospheric Research, *250*(January), 105407. https://doi.org/10.1016/j.atmosres.2020.105407
42. Santiago, J. P., & Sharkey, T. D. (2019). Pollen development at high temperature and role of carbon and nitrogen metabolites. Plant Cell and Environment, *42*(10), 2759–2775. https://doi.org/10.1111/pce.13576
43. Schmidt, C. W. (2016). Pollen Overload. Environmental Health Perspectives, *124*(4), 70–75.
44. Selinski, J., & Scheibe, R. (2014). Pollen tube growth: Where does the energy come from? Plant Signaling and Behavior, *9*(12), e977200-1-e977200-9. https://doi.org/10.4161/15592324.2014.977200
45. Subiza, J., Cabrera, M., M, C. R. J., Craciunesco, C., Narganes, M. J., & Subiza, C. (2019). *Influence of climate change on pollen counts and pollinosis in Madrid, a study over 40 years* . 78.
46. Thomson, A. M., Calvin, K. V., Smith, S. J., Kyle, G. P., Volke, A., Patel, P., Delgado-Arias, S., Bond-Lamberty, B., Wise, M. A., Clarke, L. E., & Edmonds, J. A. (2011). RCP4.5: A pathway for stabilization of radiative forcing by 2100. Climatic Change, *109*(1), 77–94. https://doi.org/10.1007/s10584-011-0151-4
47. Traidl-Hoffmann, C., Mariani, V., Hochrein, H., Karg, K., Wagner, H., Ring, J., Mueller, M. J., Jakob, T., & Behrendt, H. (2005). Pollen-associated phytoprostanes inhibit dendritic cell interleukin-12 production and augment T helper type 2 cell polarization. Journal of Experimental Medicine, *201*(4), 627–635. https://doi.org/10.1084/jem.20041065
48. Valone, T. F. (2021). Linear Global Temperature Correlation to Carbon Dioxide Level,Sea Level, and Innovative Solutions to a Projected 6°C Warming by 2100. *Journal of Geoscience and Environment Protection*, *09*(03), 84–135. https://doi.org/10.4236/gep.2021.93007
49. van Proosdij, A. S. J., Sosef, M. S. M., Wieringa, J. J., & Raes, N. (2016). Minimum required number of specimen records to develop accurate species distribution models. Ecography, *39*(6), 542–552. https://doi.org/10.1111/ecog.01509
50. Whistler, W. A., & Elevitch, C. R. (2006). Broussonetia papyrifera (paper mulberry). Species Profiles for Pacific Island Agroforestry, *April*, 1–13.
51. Whitney, B. S., & Needham, T. (2014). Isopropyl alcohol: A replacement for tertiary-butyl alcohol in pollen preparations. Review of Palaeobotany and Palynology, *203*, 9–11. https://doi.org/10.1016/j.revpalbo.2013.11.004
52. Wu, P. C., Su, H. J., Lung, S. C. C., Chen, M. J., & Lin, W. P. (2019). Pollen of Broussonetia papyrifera: An emerging aeroallergen associated with allergic illness in Taiwan. Science of the Total Environment, *657*, 804–810. https://doi.org/10.1016/j.scitotenv.2018.11.324

53. Yang, Y. L., & Chen, S. H. (1998). An investigation of Airborne pollen in Taipei City, Taiwan, 1993–1994. Journal of Plant Research, *111*(4), 501–508. https://doi.org/10.1007/bf02507785

54. Zeghoud, S., Rebiai, A., Hemmami, H., Ben Seghir, B., Elboughdiri, N., Ghareba, S., Ghernaout, D., & Abbas, N. (2021). ATR-FTIR Spectroscopy, HPLC Chromatography, and Multivariate Analysis for Controlling Bee Pollen Quality in Some Algerian Regions. ACS Omega, *6*(7), 4878–4887. https://doi.org/10.1021/acsomega.0c05816

55. Ziello, C., Sparks, T. H., Estrella, N., Belmonte, J., Bergmann, K. C., Bucher, E., Brighetti, M. A., Damialis, A., Detandt, M., Galán, C., Gehrig, R., Grewling, L., Bustillo, A. M., Hallsdóttir, M., Kockhans-Bieda, M. C., Linares, de C., Myszkowska, D., Pàldy, A., Sánchez, A., … Menzel, A. (2012). Changes to airborne pollen counts across europe. *PLoS ONE*, *7*(4). https://doi.org/10.1371/journal.pone.0034076

56. Zimmermann, B., Bağcıoğlu, M., Tafinstseva, V., Kohler, A., Ohlson, M., & Fjellheim, S. (2017). *Original Research A high- throughput FTIR spectroscopy approach to assess adaptive variation in the chemical composition of pollen*. *July*, 10839–10849. https://doi.org/10.1002/ece3.3619

57. Zimmermann, B., & Kohler, A. (2014). *Infrared Spectroscopy of Pollen Identifies Plant Species and Genus as Well as Environmental Conditions*. *9*(4). https://doi.org/10.1371/journal.pone.0095417

Figures

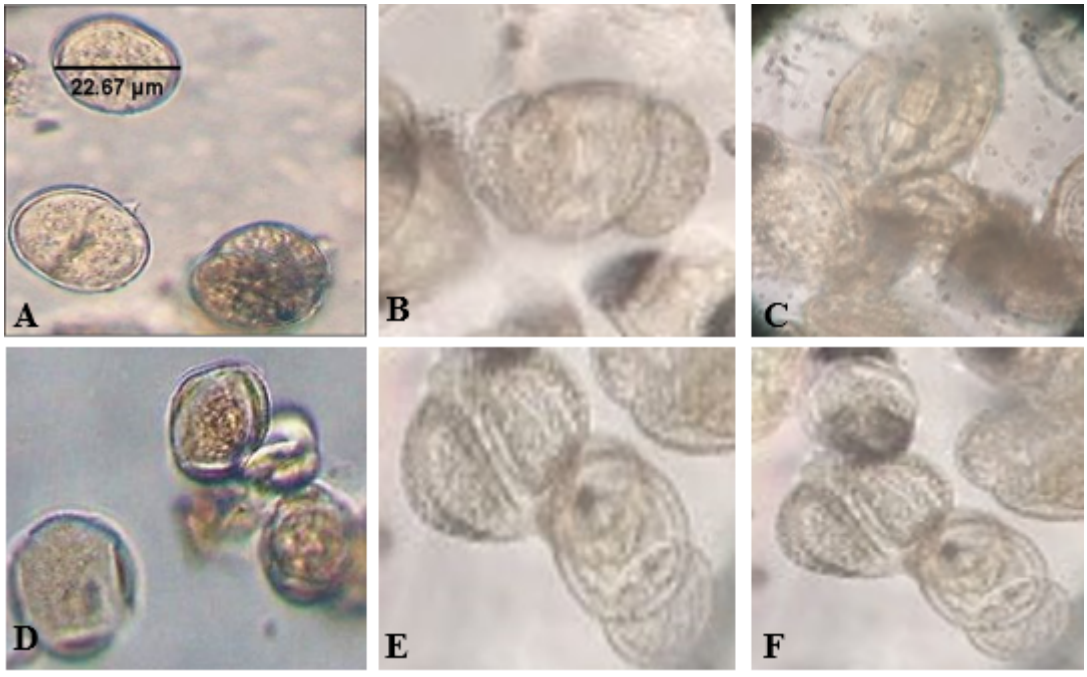

Figure 1

Light microscope images of B. papyriferapollen captured at 100 X A) pollen collected from R1, B) pollen collected from R2, C) pollen collected from R3 in spring 2020. D) pollen collected from R1, E) collected from R2, C) collected from R3 in spring 2021.

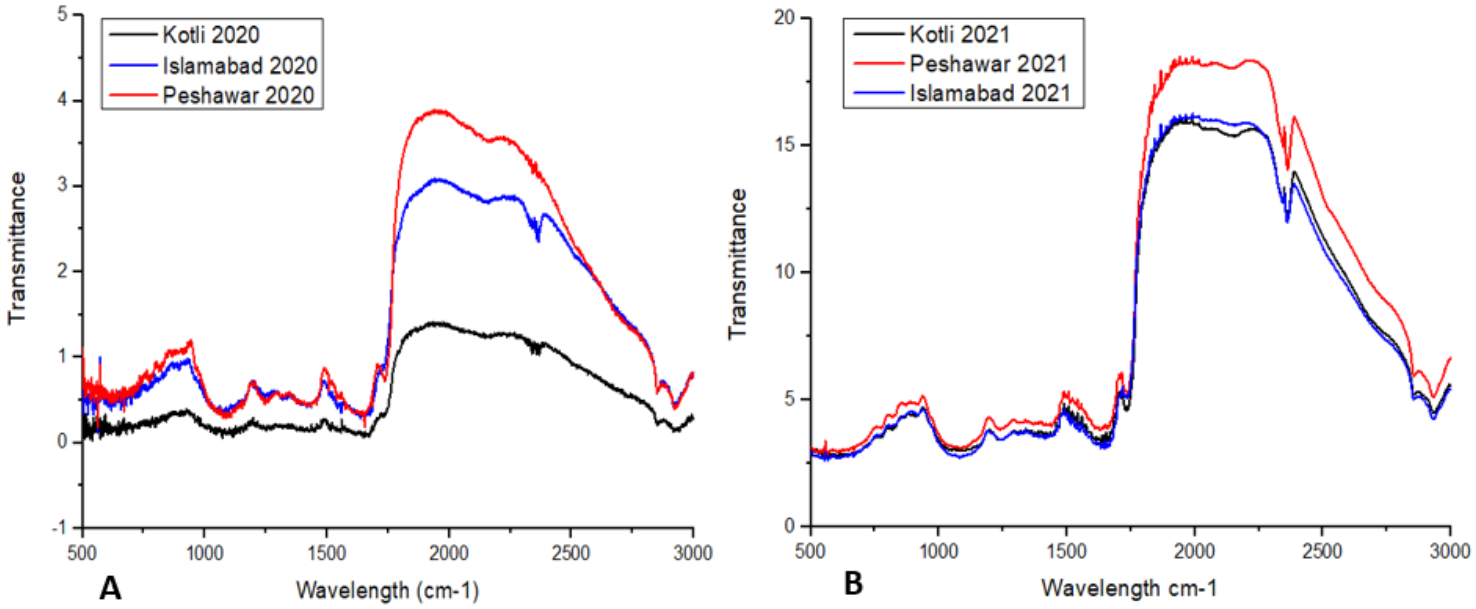

Figure 2

Broussonetia Papyriferainter–regional pollen FTIR analysis Red, blue and black bar lines denote R1, R2 and R3 A) Shows pollen spectra of samples collected in spring of 2020. B) Shows pollen spectra of samples collected in the spring of 2021.

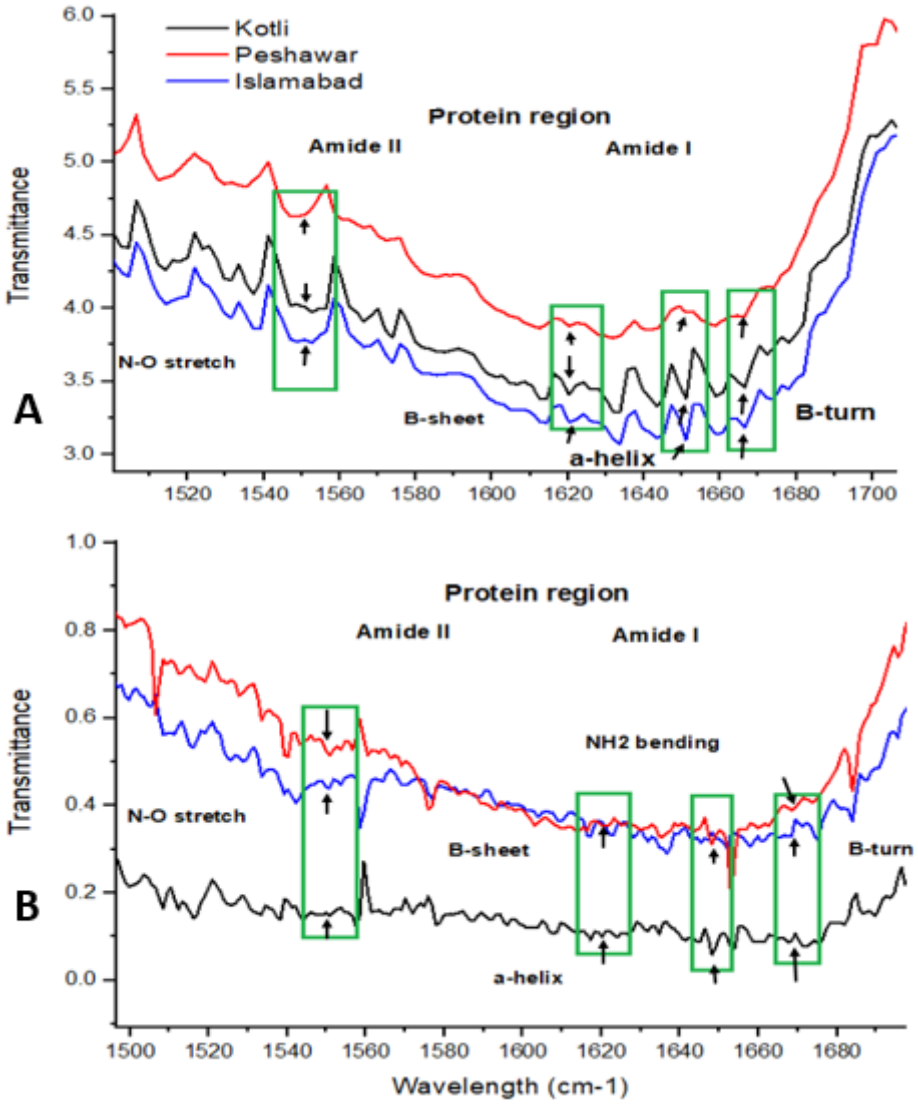

Figure 3

Location effect on FTIR spectra of pollen protein content collected in the spring 2020 and spring 2021 A) Shows protein spectra of R1, R2 and R3 for pollen collected in 2021. B) Protein spectra of R1, R2 and R3 pollen sampled in spring 2020.

Lipid region has variation in peak intensities in 2020 for CH_2 and CH_3 functional groups at 2850 cm^{-1} and 2930 cm^{-1} for R1, R2 and R3 (Fig. 4A and Fig. 4B). The pollens of same region have lost peak intensities in 2021. These variations in spectral peaks reflect differences in weather conditions impact on pollen structures.

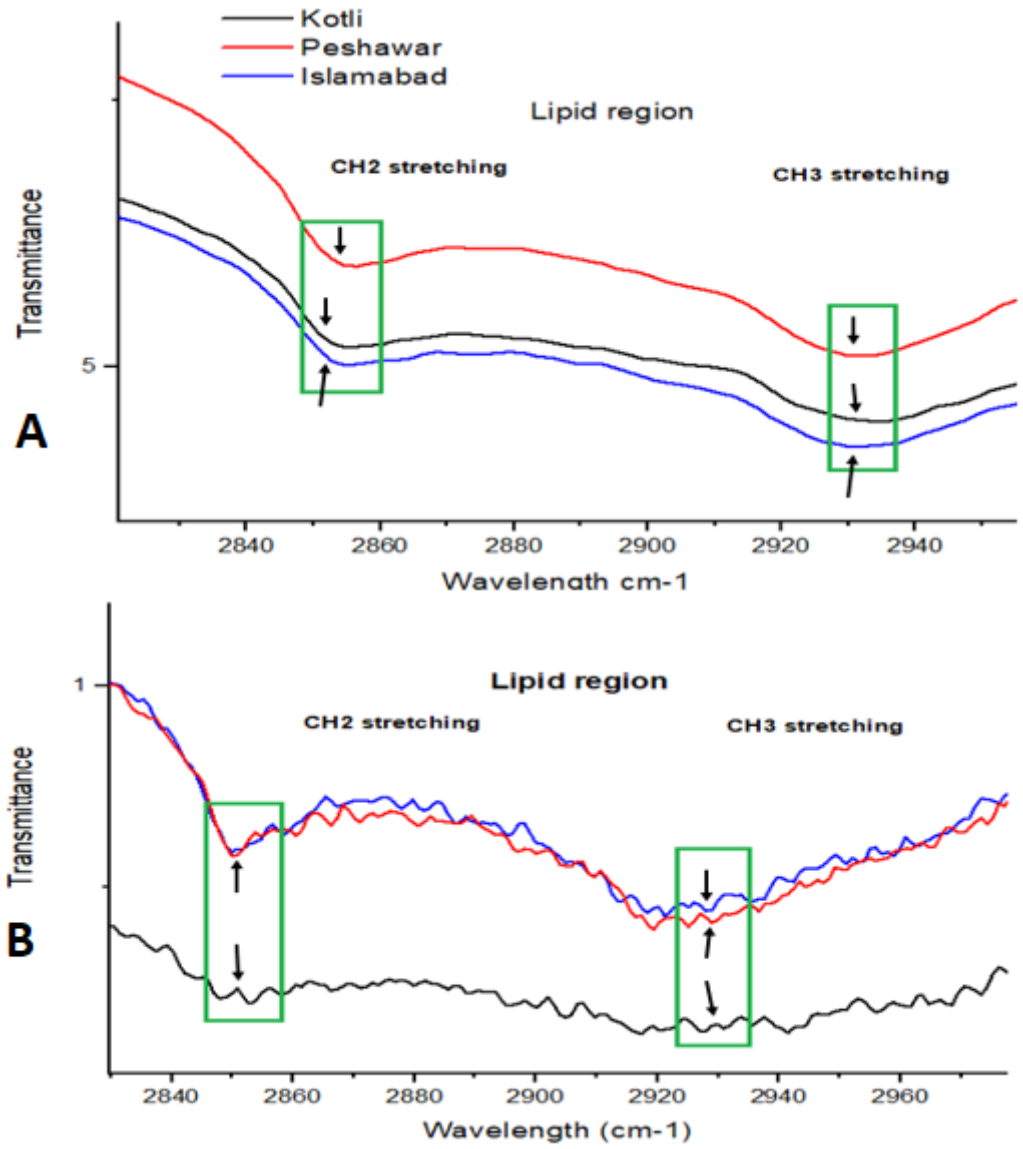

Figure 4

Seasonal and climatic effects on lipid region of pollen A) Shows spring 2021 pollen FTIR spectra for lipid region 2840 cm^{-1} to 2940 cm^{-1}. B) Show spring 2020 pollen FTIR spectra for lipid region 2840 cm^{-1} to 2940 cm^{-1}.

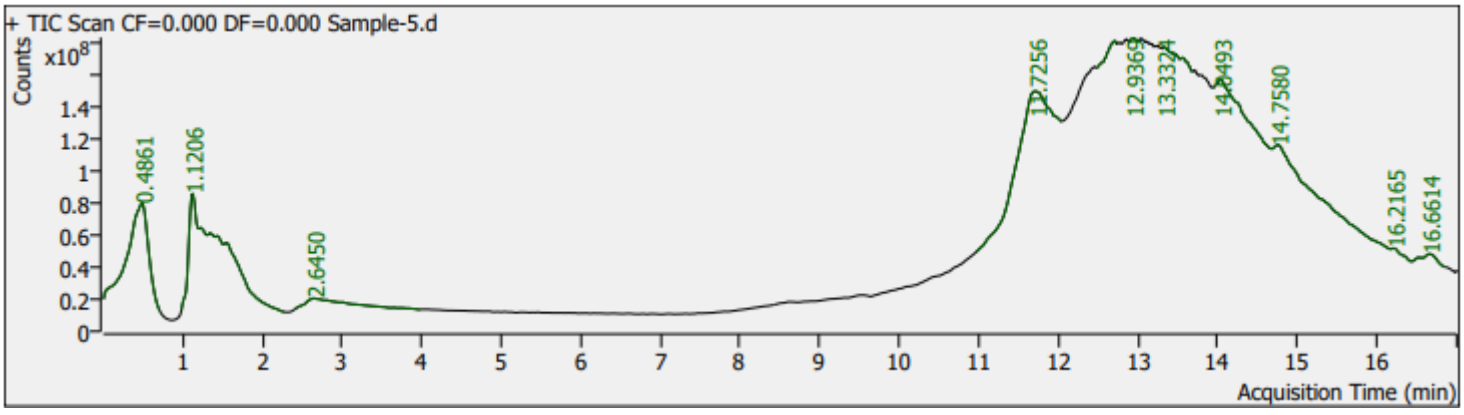

Figure 5

LCMS analysis of B. papyrifera pollen. Y-axis shows charge to mass ratio for the ions of various compounds separated at different time intervals while the X-axis denotes acquisition time in minutes. The sample run time is 16 min having the highest peak at 13th minute 12.9369. The analysis shows the variance in charge to mass ratios of ions present in the pollen that make unique peaks. Peaks analysis shows the presence of different compounds in the analysed pollen (for details see S1Table).

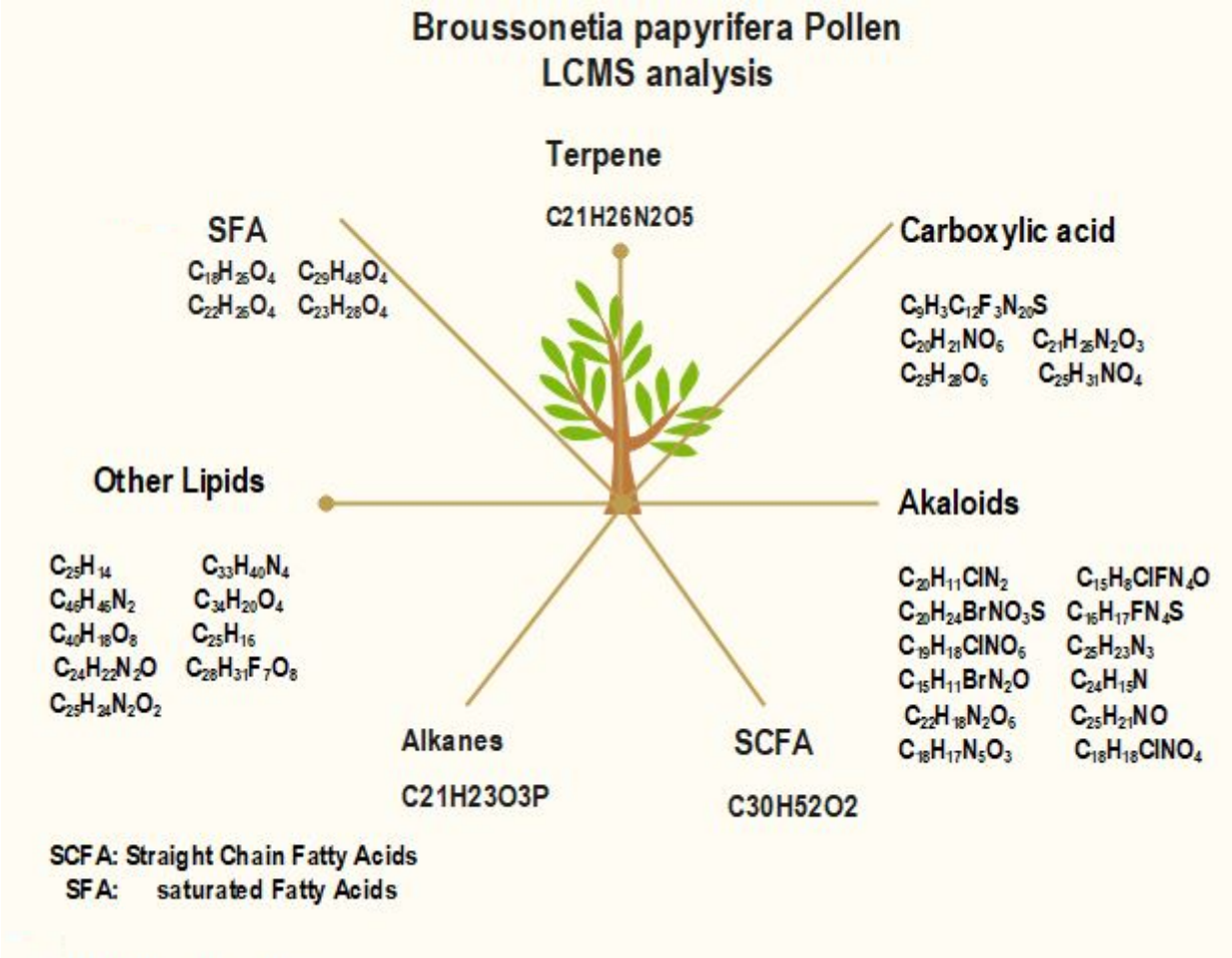

Figure 6

Schematic distribution of organic compounds in B. papyrifera pollen grains by LCMS analysis. Total compounds identified in the pollen samples are classified into 7 groups: alkanes, alkaloids, carboxylic acids, terpenes, other lipids, straight-chain fatty acids, and unsaturated fatty acids (USFA). USFA marked in red color shows the presence of allergenic compounds in the pollen grains of B. papyrifera.

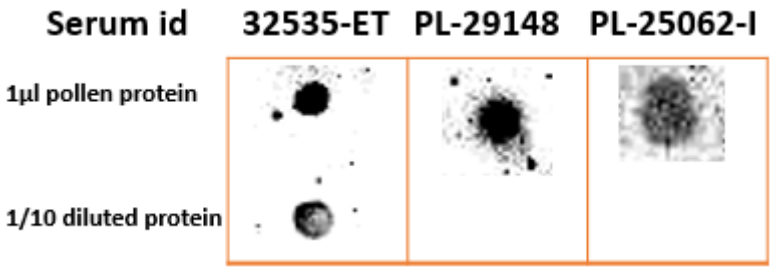

Figure 7

Dot blot of *B. papyrifera* pollen-protein extract. 1µl of pure pollen-protein extracts and 1/10 diluted pollen-protein extracts in 1X PBS blotted on a nitrocellulose paper against 1:1000 diluted anti IgE monoclonal HRP Southern Biotech antibodies. The dark spots show IgE binding with the respective serum id given above the spot.

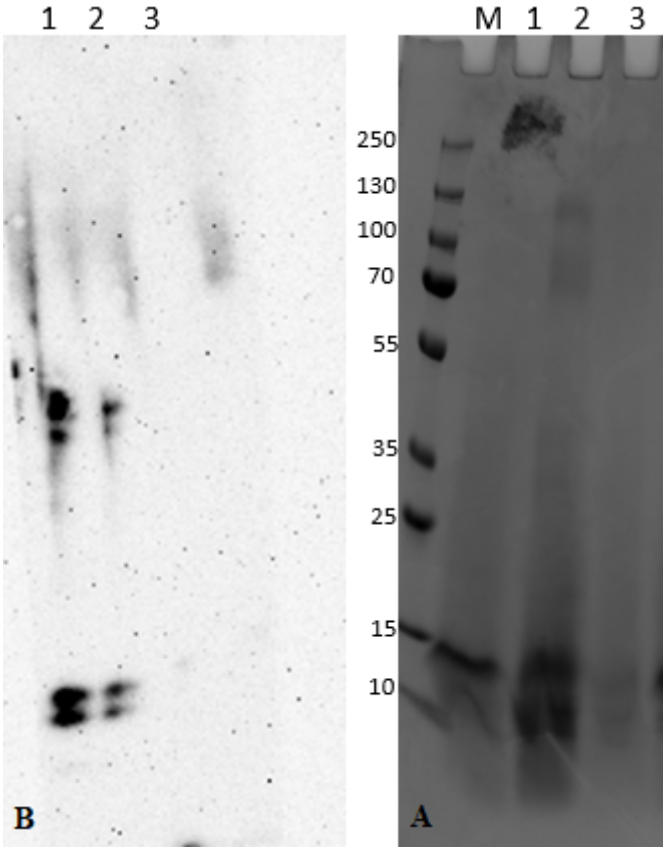

Figure 8

Western blot analysis of *B. papyrifera*-pollen protein. A) shows *B. papyrifera*-pollen protein on a stained gel with 250 kDa pre-stained Precision Plus molecular weight marker proteins. B) shows western blotting image of allergens on nitrocellulose membrane. The western blot analysis depicts 4 bands in lane 1 and lane 2 having primary antibody binding with 1:1000 diluted secondary antibodies.

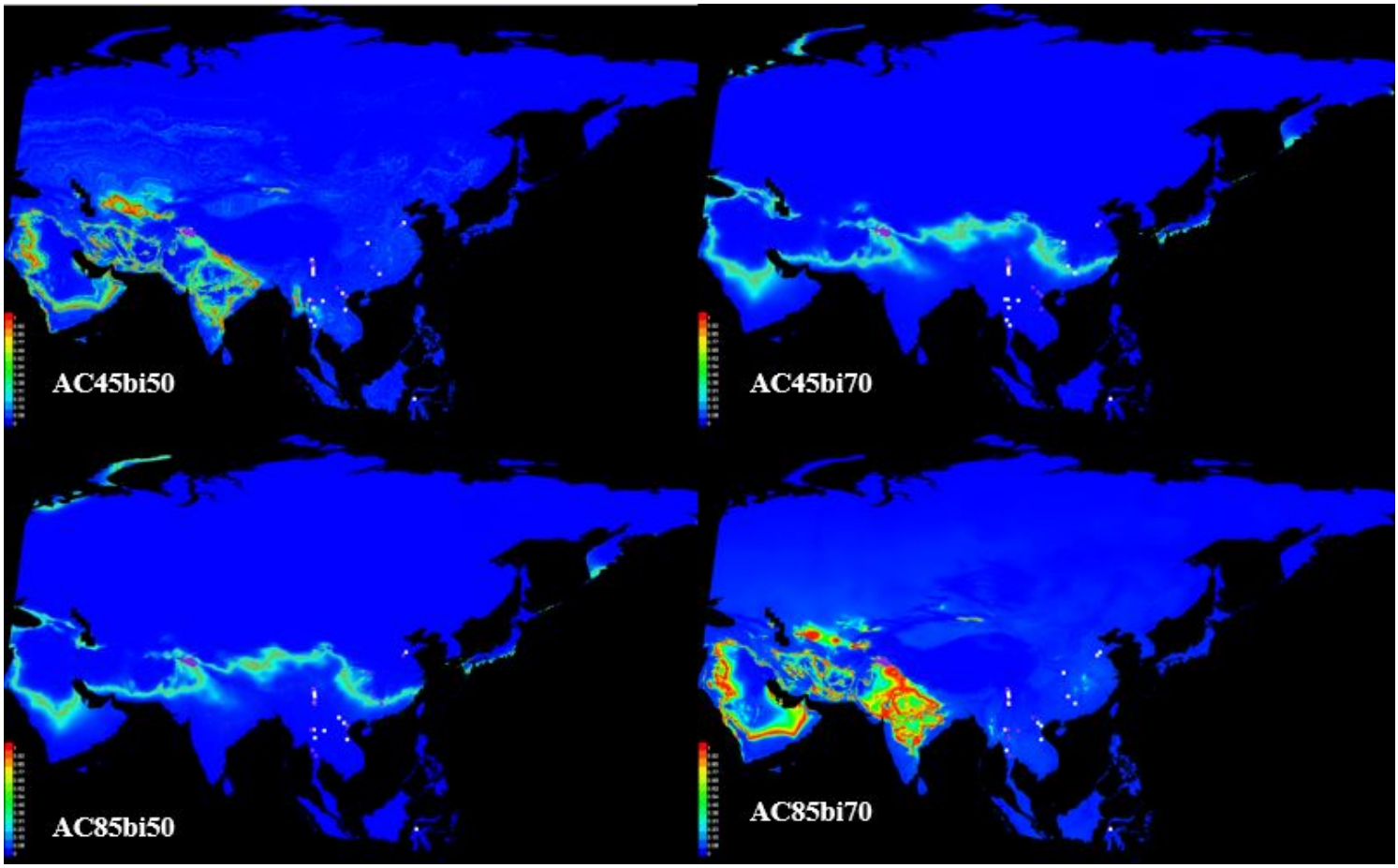

Figure 9

ACCESS1.0 based MaxEnt modeling of *B. papyrifera*growth occurrence in the years 2050 and 2070 in Asia. The Fig. shows *B. papyrifera* perspective future distribution in the years 2050 and 2070 through ACCESS1.0 CMIP5 dataset. AC represents ACCESS, 4.5 shows representative climate change pathway (RCP) 4.5, 8.5 shows representative climate change pathway (RCP) 8.5, and bi50 and bi70 denote bioclimatic variables in the year 2050 and 2070. White and blue squares on the map show occurrence points of *B. papyrifera*used in the MaxEnt modeling while the colored scale (0-1) on the right side of the map shows the suitability of locations for *B. papyrifera* growth invasion in the future.

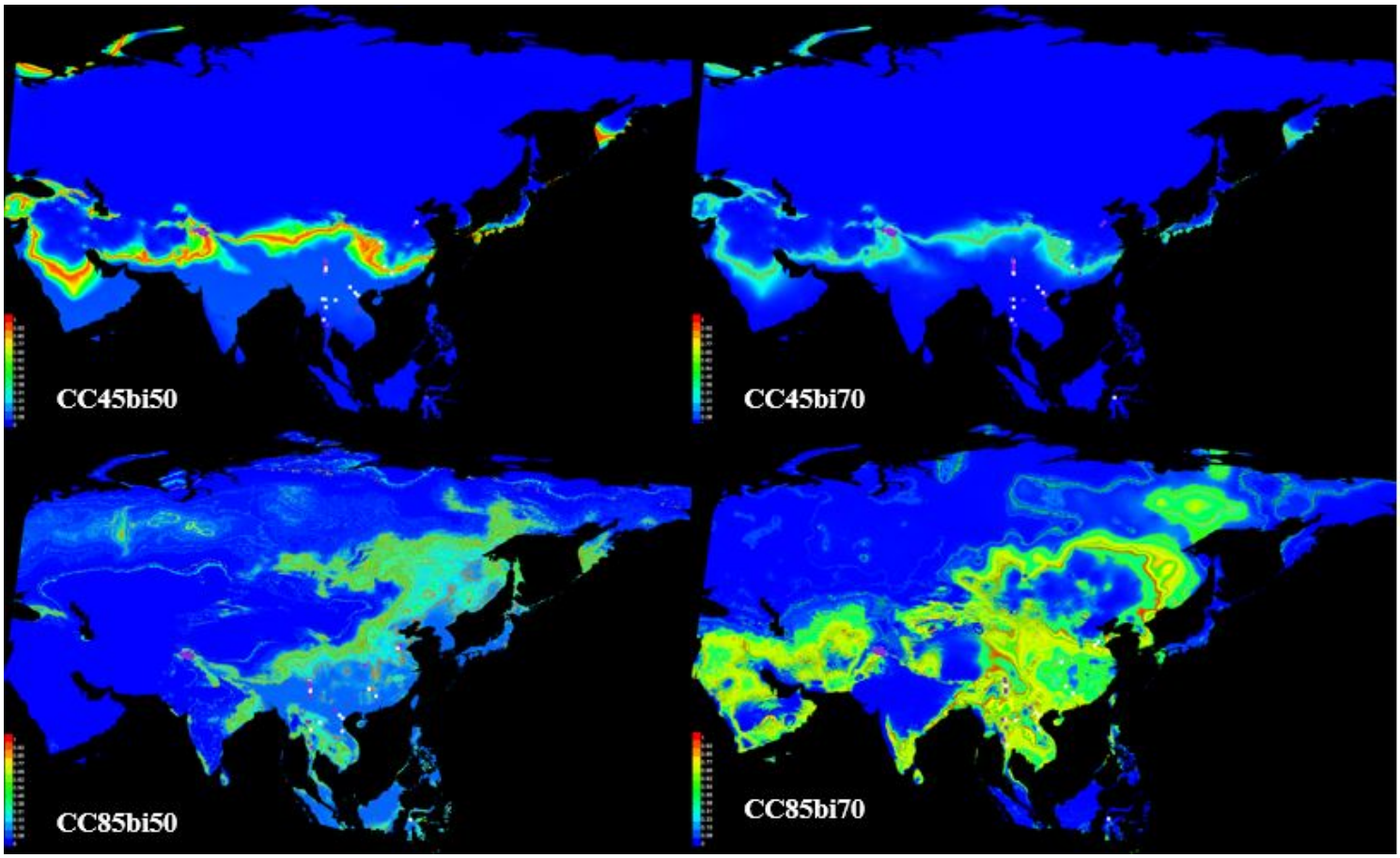

Figure 10

CCSM4 based MaxEnt modeling of *B. papyrifera* growth occurrence in the years 2050 and 2070 in Asia. The Fig. shows *B. papyrifera*'s prospective future distribution in the years 2050 and 2070 through the CCSM4 CMIP5 dataset. CC represents CCSM4, 4.5 shows representative climate change pathway (RCP) 4.5, 8.5 shows representative climate change pathway (RCP) 8.5, and bi50 and bi70 denotes bioclimatic variables in the year 2050 and 2070. White and blue squares on the map show occurrence points of *B. papyrifera* used in the MaxEnt modeling while the colored scale (0-1) on the right side of the map shows the suitability of locations for *B. papyrifera* growth invasion in the future.

Supplementary Files

This is a list of supplementary files associated with this preprint. Click to download.

- S1Fig.MeanannualprecipitationofR1R2andR3.tiff
- S2Fig.MeanannualtemperatureofR1R2andR3.tiff
- S3Fig.Springsingledaymaximumpollencountin1cubicmeterinR2.tiff